

Neutral-current SMEFT studies at the EIC

Kağan Şimşek

Northwestern
University

in collaboration with

Radja Boughezal, Alexander Emmert, Tyler Kutz, Sonny Mantry,
Michael Nycz, Frank Petriello, Daniel Wiegand, and Xiaochao Zheng

reference: arXiv:2204.07557

CFNS Workshop: High-Luminosity EIC

June 21, 2022

Introduction

Introduction

- The SM of particle physics has been successful in describing all lab phenomena.
- Yet it has shortcomings:
 - * no explanation for dark matter, baryon-antibaryon asymmetry, or neutrino mass
 - * the hierarchy problem
- Many models beyond the SM have been proposed to address these issues.

Introduction

- No evidence for new particles beyond the predicted spectrum has been found yet.
- We follow the SMEFT framework to parameterize the BSM effects.
- Higher-dimensional operators are built of existing SM particles:

$$\mathcal{L}_{\text{SMEFT}} = \mathcal{L}_{\text{SM}} + \sum_{n>4} \frac{1}{\Lambda^{n-4}} \sum_k C_k^{(n)} O_k^{(n)}$$

- All new physics is assumed to be heavier than SM states and accessible collider energy.
- We focus on $n = 6$ and semi-leptonic 4-fermion $O_k^{(n)}$.
- We study NC DIS cross-section asymmetries at EIC.
- We find that the EIC can
 - * probe complementary and competitive to LHC DY
 - * resolve degeneracies observed in LHC NC DY data

Outline

Part I: Neutral-current DIS and SMEFT

Part II: Data analysis

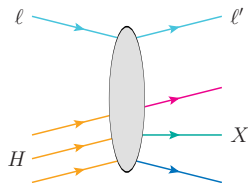
Part III: SMEFT fit results

Neutral-current DIS and SMEFT

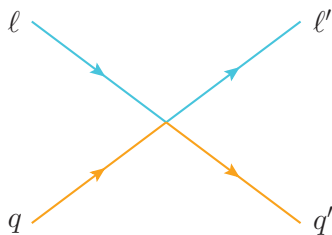
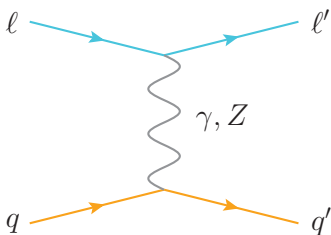
NC DIS and SMEFT

We study the DIS in the process

$$\ell + H \rightarrow \ell' + X$$



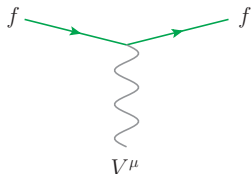
which is, at parton level, mediated by a photon or Z boson exchange in the NC case or a contact interaction of two leptons and two quarks:



NC DIS and SMEFT

Parameterize the vertex factors in terms of vector and axial couplings:

- ffV vertex consists of the usual SM coupling and SMEFT shifts characterized by Wilson coefficients, C_k :

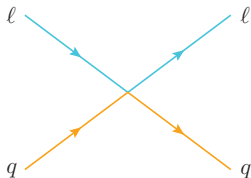


$$i\gamma_\mu g_1^{(fV)} + i\gamma_\mu \gamma_5 g_5^{(fV)}$$

SMEFT operators shift the usual vector and axial couplings, e.g.

$g_1^{(fZ)} = g_V^f + \mathcal{O}(C_k)$ and $g_5^{(fZ)} = g_A^f + \mathcal{O}(C_k)$, in a gauge-invariant way.

- $llqq$ vertex is entirely SMEFTical:



$$i[\gamma_\mu][\gamma^\mu]g_{11}^{(\ell q)} + i[\gamma_\mu][\gamma^\mu \gamma_5]g_{15}^{(\ell q)} \\ + i[\gamma_\mu \gamma_5][\gamma^\mu]g_{51}^{(\ell q)} + i[\gamma_\mu \gamma_5][\gamma^\mu \gamma_5]g_{55}^{(\ell q)}$$

SMEFT operators

Operators that contribute to the ffV and $\ell\ell qq$ vertices at dimension 6 are (Grzadkowski *et al.* [[1008.4884](#)]):

ffV	$\ell\ell qq$
$O_{\phi\ell}^{(1)} = (\varphi^\dagger i \overleftrightarrow{D}_\mu \varphi)(\bar{\ell}\gamma^\mu \ell)$	$O_{\ell q}^{(1)} = (\bar{\ell}\gamma_\mu \ell)(\bar{q}\gamma^\mu q)$
$O_{\phi\ell}^{(3)} = (\varphi^\dagger i \overleftrightarrow{D}_\mu \tau^I \varphi)(\bar{\ell}\gamma^\mu \tau^I \ell)$	$O_{\ell q}^{(3)} = (\bar{\ell}\gamma_\mu \tau^I \ell)(\bar{q}\gamma^\mu \tau^I q)$
$O_{\phi e} = (\varphi^\dagger i \overleftrightarrow{D}_\mu \varphi)(\bar{e}\gamma^\mu e)$	$O_{eu} = (\bar{e}\gamma_\mu e)(\bar{u}\gamma^\mu u)$
$O_{\phi q}^{(1)} = (\varphi^\dagger i \overleftrightarrow{D}_\mu \varphi)(\bar{q}\gamma^\mu q)$	$O_{ed} = (\bar{e}\gamma_\mu e)(\bar{d}\gamma^\mu d)$
$O_{\phi q}^{(3)} = (\varphi^\dagger i \overleftrightarrow{D}_\mu \tau^I \varphi)(\bar{q}\gamma^\mu \tau^I q)$	$O_{lu} = (\bar{\ell}\gamma_\mu \ell)(\bar{u}\gamma^\mu u)$
$O_{\phi u} = (\varphi^\dagger i \overleftrightarrow{D}_\mu \varphi)(\bar{u}\gamma^\mu u)$	$O_{ld} = (\bar{\ell}\gamma_\mu \ell)(\bar{d}\gamma^\mu d)$
$O_{\phi d} = (\varphi^\dagger i \overleftrightarrow{D}_\mu \varphi)(\bar{d}\gamma^\mu d)$	$O_{qe} = (\bar{q}\gamma_\mu q)(\bar{e}\gamma^\mu e)$

There is one more:

$$O_{\phi WB} = (\varphi^\dagger \tau^I \varphi) W_{\mu\nu}^I B^{\mu\nu} \Rightarrow \text{causes kinetic mixing of } W^3 \text{ and } B$$

\Rightarrow universally shifts the ffV vertices after

diagonalization of photon and Z boson states

SMEFT operators

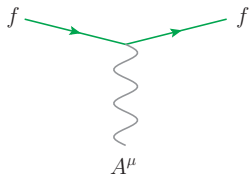
The ffV operators are already strongly bounded by Z and W pole observables (Dawson & Giardino [1909.02000]):

C_k	95% CL, $\Lambda = 1$ TeV
$C_{\varphi\ell}^{(1)}$	$[-0.043, 0.012]$
$C_{\varphi\ell}^{(3)}$	$[-0.012, 0.0029]$
$C_{\varphi e}$	$[-0.013, 0.0094]$
$C_{\varphi q}^{(1)}$	$[-0.027, 0.043]$
$C_{\varphi q}^{(3)}$	$[-0.011, 0.014]$
$C_{\varphi u}$	$[-0.072, 0.091]$
$C_{\varphi d}$	$[-0.16, 0.060]$
$C_{\varphi WB}$	$[-0.0088, 0.0013]$

Thus, we restrict our attention only to the operators contributing to the $\ell\ell qq$ vertex, which leaves us with seven Wilson coefficients of interest: $C_{e\ell}$, C_{ed} , $C_{\ell q}^{(1)}$, $C_{\ell q}^{(3)}$, $C_{\ell u}$, $C_{\ell d}$, and C_{qe} .

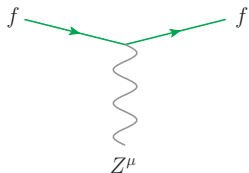
Vertex factors

Since we consider contributions only to the $llqq$ interaction, we assume the usual ffV vertices in our analysis:



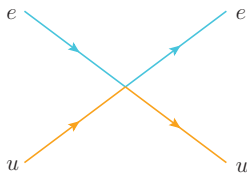
$$g_1^{(fA)} = -eQ_f$$

$$g_5^{(fA)} = 0$$



$$g_1^{(fZ)} = g_V^f$$

$$g_5^{(fZ)} = g_A^f$$

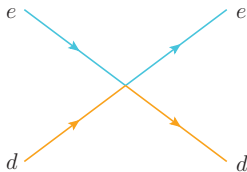


$$g_{11}^{(eu)} = \frac{1}{4} [C_{eu} + (C_{\ell q}^{(1)} - C_{\ell q}^{(3)}) + C_{\ell u} + C_{qe}]$$

$$g_{15}^{(eu)} = \frac{1}{4} [C_{eu} - (C_{\ell q}^{(1)} - C_{\ell q}^{(3)}) + C_{\ell u} - C_{qe}]$$

$$g_{51}^{(eu)} = \frac{1}{4} [C_{eu} - (C_{\ell q}^{(1)} - C_{\ell q}^{(3)}) - C_{\ell u} + C_{qe}]$$

$$g_{55}^{(eu)} = \frac{1}{4} [C_{eu} + (C_{\ell q}^{(1)} - C_{\ell q}^{(3)}) - C_{\ell u} - C_{qe}]$$



the same as for $eeuu$ but with $u \rightarrow d$ and $C_{\ell q}^{(1)} - C_{\ell q}^{(3)} \rightarrow C_{\ell q}^{(1)} + C_{\ell q}^{(3)}$

Partonic cross section

Total amplitude for $\ell + q \rightarrow \ell' + q'$:

$$\mathcal{M} = \mathcal{M}_\gamma + \mathcal{M}_Z + \mathcal{M}_\times$$

Total amplitude squared:

$$|\mathcal{M}|^2 = \mathcal{M}_{\gamma\gamma} + \mathcal{M}_{ZZ} + \mathcal{M}_{\gamma Z} + \mathcal{M}_{\gamma\times} + \mathcal{M}_{Z\times} + \mathcal{O}(C^2)$$

Partonic cross section:

$$d\sigma = \frac{d^2\sigma}{dx dQ^2} = \frac{1}{16\pi x^2 s^2} |\mathcal{M}|^2$$

Make helicity-dependence explicit:

$$d\sigma = d\sigma^{\lambda_\ell \lambda_q}$$

Asymmetries

Three types of asymmetries:

- lepton left-right asymmetries of unpolarized hadrons:
unpolarized PV asymmetries, A_{PV}
- hadron left-right asymmetries with unpolarized leptons:
polarized PV asymmetries, ΔA_{PV}
- unpolarized e^-e^+ asymmetries of unpolarized hadrons:
lepton-charge asymmetries, A_{LC}

Asymmetries

Various cross sections entering asymmetries:

- unpolarized lepton + unpolarized hadron:

$$d\sigma_0 = \frac{1}{4} \sum_q f_{q/H} [d\sigma^{++} + d\sigma^{+-} + d\sigma^{-+} + d\sigma^{--}]$$

- polarized lepton + unpolarized hadron:

$$d\sigma_\ell = \frac{1}{4} \sum_q f_{q/H} [d\sigma^{++} + d\sigma^{+-} - d\sigma^{-+} - d\sigma^{--}]$$

- unpolarized lepton + polarized hadron:

$$d\sigma_H = \frac{1}{4} \sum_q \Delta f_{q/H} [d\sigma^{++} - d\sigma^{+-} + d\sigma^{-+} - d\sigma^{--}]$$

Active quark flavors: $q \in \{u, \bar{u}, d, \bar{d}, s, \bar{s}\}$

Asymmetries

Asymmetry definitions:

- unpolarized PV asymmetries:

$$A_{\text{PV}} = \frac{d\sigma_{\ell}}{d\sigma_0}$$

- polarized PV asymmetries:

$$\Delta A_{\text{PV}} = \frac{d\sigma_H}{d\sigma_0}$$

- lepton-charge asymmetries:

$$A_{\text{LC}} = \frac{d\sigma_0(e^+H) - d\sigma_0(e^-H)}{d\sigma_0(e^+H) + d\sigma_0(e^-H)}$$

Data analysis

Projection of asymmetry data

Preliminary EIC data:

- simulations with Djangoh Monte-Carlo event generator
- including full EW radiative events
- data across x and Q bins
- smearing of full-detector simulated events
- e^- event count from σ and \mathcal{L}

Important points:

- (1) bin migration and unfolding: due to radiative effects
- (2) background radiation: due to final-state hadron

Remark: The full details of the simulation only matter for the SMEFT part at the 20-30% level.

Event selection

Cuts on projected data:

$Q > 1 \text{ GeV}$ to avoid nonperturbative region of QCD

$y > 0.1$ to avoid bin migration and unfolding uncertainty

$y < 0.9$ to avoid high photoproduction background due to final-state hadron

$|\eta| < 3.5$ to restrict events in main acceptance of ECCE detector

$E' > 2 \text{ GeV}$ to ensure e^- samples with high purity

Additional cuts in SMEFT analysis:

$x < 0.5$ } to avoid large uncertainties from
 $Q > 10 \text{ GeV}$ } nonperturbative QCD and nuclear dynamics

Data sets

Data sets used in our analysis, shown with beam energies and nominal annual luminosities:

D1	5 GeV \times 41 GeV <i>eD</i> , 4.4 fb ⁻¹	P1	5 GeV \times 41 GeV <i>ep</i> , 4.4 fb ⁻¹
D2	5 GeV \times 100 GeV <i>eD</i> , 36.8 fb ⁻¹	P2	5 GeV \times 100 GeV <i>ep</i> , 36.8 fb ⁻¹
D3	10 GeV \times 100 GeV <i>eD</i> , 44.8 fb ⁻¹	P3	10 GeV \times 100 GeV <i>ep</i> , 44.8 fb ⁻¹
D4	10 GeV \times 137 GeV <i>eD</i> , 100 fb ⁻¹	P4	10 GeV \times 275 GeV <i>ep</i> , 100 fb ⁻¹
D5	18 GeV \times 137 GeV <i>eD</i> , 15.4 fb ⁻¹	P5	18 GeV \times 275 GeV <i>ep</i> , 15.4 fb ⁻¹
		P6	18 GeV \times 275 GeV <i>ep</i> , 100 fb ⁻¹

P6: Yellow Report reference setting [2103.05419]

Since the most interesting results are obtained with the low-energy high-luminosity 4th and high-energy low-luminosity 5th sets, highlighted by red, we restrict our attention to these.

We take copies of these data sets by labeling them ΔD and ΔP for polarized PV asymmetries and LD and LP for lepton-charge asymmetries.

Statistical uncertainty projections for PV asymmetries

For a given value of integrated luminosity:

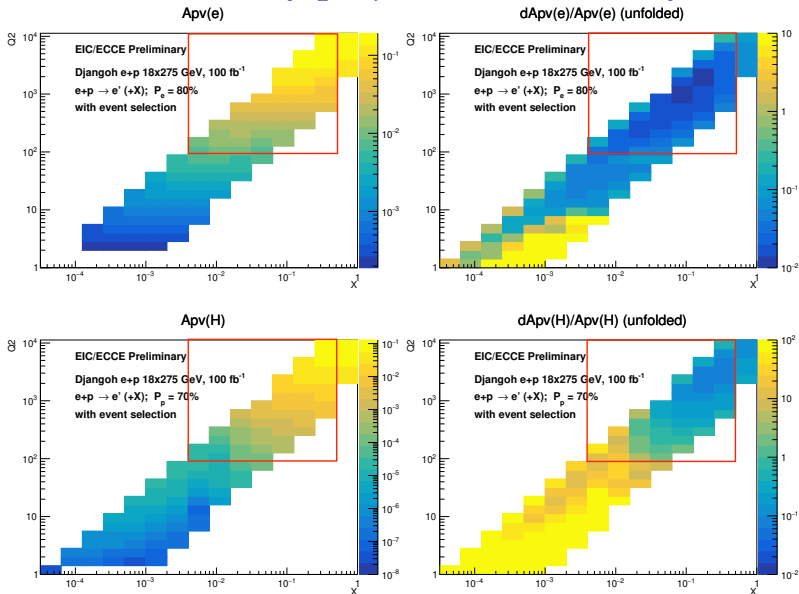
$$\delta A_{\text{stat}} = \frac{1}{\sqrt{N}} \xrightarrow{\text{PV asymmetries}} \frac{1}{|P|} \frac{1}{\sqrt{N}}$$

Assumed reaches of beam polarization:

$$P_{\ell} = 80\% \text{ with } 1\% \text{ rel. sys. error}$$

$$P_H = 70\% \text{ with } 2\% \text{ rel. sys. error}$$

Statistical uncertainty projections for PV asymmetries



The red boxes indicate the region of the phase space considered in our SMEFT analysis.

Uncertainty projections for LC asymmetries

For the LC asymmetries, we would have two different runs for e^- and e^+ :

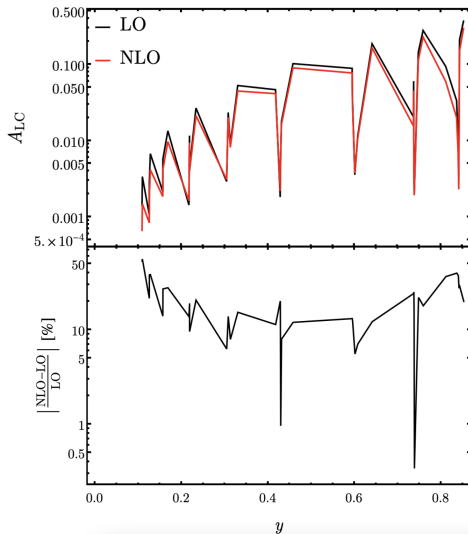
- The dominant uncertainty would come from the $e^- - e^+$ luminosity difference, which we assume to be 2% relative.
- We introduce this value as an absolute luminosity uncertainty in A_{LC} , i.e. $[\delta A_{LC}]_{\text{lum}} = 0.02$.

Since we compare cross sections with two different leptons, there may be sizable differences in higher-order corrections:

- QCD NLO corrections to A_{LC} are small.
- QED NLO corrections to A_{LC} are about 10% relative to the LO values.

QED NLO corrections to A_{LC}

e.g. ep collision with $10 \text{ GeV} \times 275 \text{ GeV}$, 100 fb^{-1} (the P4 data set):



Introduce 5% of the difference between NLO and LO A_{LC} values as the QED NLO uncertainty.

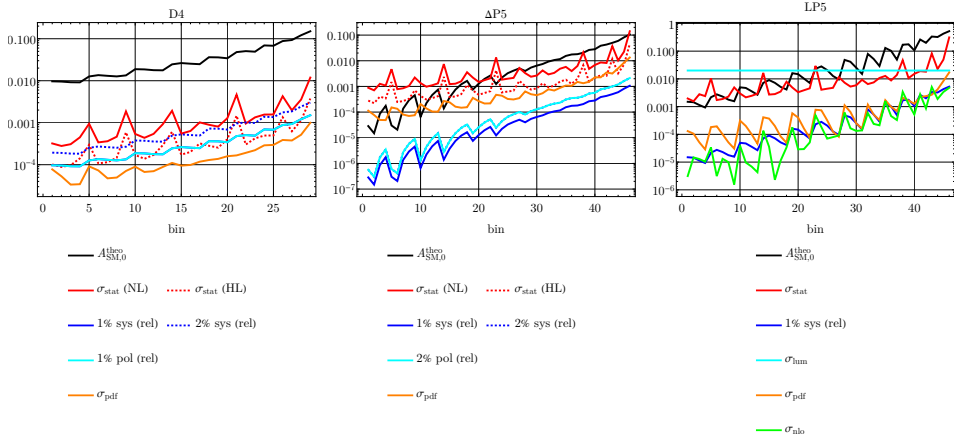
10-fold luminosity upgrade beyond initial run: Assuming everything else remains the same,

$$\sigma_{\text{stat}} \rightarrow \frac{1}{\sqrt{10}} \sigma_{\text{stat}}$$

Anticipated errors

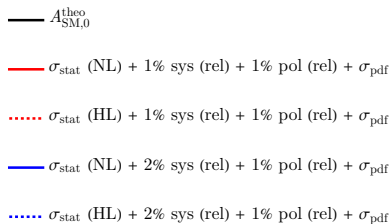
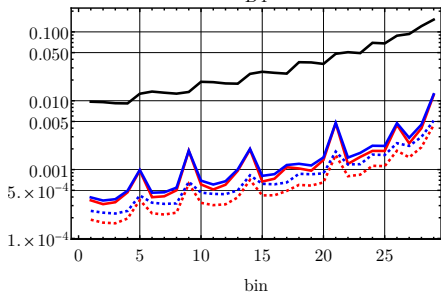
Error type	$A_{PV} (D, P)$	$\Delta A_{PV} (\Delta D, \Delta P)$	$A_{LC} (LD, LP)$
statistical	σ_{stat}	$\frac{P_\ell}{P_H} \sigma_{\text{stat}}$	$\sqrt{10} P_\ell \sigma_{\text{stat}}$
uncorrelated systematic	1% rel.	1% rel.	1% rel.
fully correlated beam polarization	1% rel.	2% rel.	✗
fully correlated luminosity	✗	✗	2% abs.
uncorrelated QED NLO	✗	✗	$5\% \times (A_{LC}^{\text{NLO}} - A_{LC}^{\text{Born}})$
fully correlated PDF	✓	✓	✓

Error budget: Uncertainty components

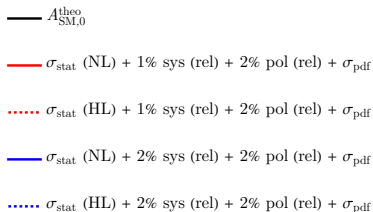
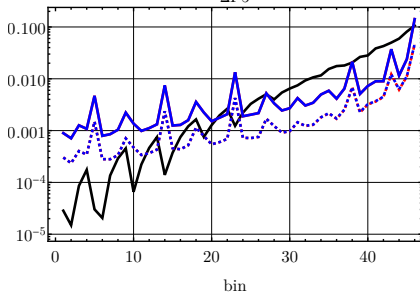


Error budget: Combined uncertainties

D4



$\Delta P5$



SMEFT analysis: Pseudodata generation

$$A_{\text{pseudo},b}^{(e)} = A_{\text{SM},b} + r_b^{(e)} \sigma_b^{\text{unc}} + r'^{(e)} \sigma_b^{\text{cor}}$$

Bin and pseudoexperiment indices:

$$b \in \text{Range}(N_{\text{bin}}), \quad e \in \text{Range}(N_{\text{exp}}), \quad N_{\text{exp}} = 10^3$$

For PV asymmetries:

$$\sigma_b^{\text{unc}} = \sigma_{\text{stat},b} \oplus \sigma_{\text{sys},b}$$

$$\sigma_b^{\text{cor}} = \sigma_{\text{pol},b}$$

For LC asymmetries:

$$\sigma_b^{\text{unc}} = \sigma_{\text{stat},b} \oplus \sigma_{\text{sys},b} \oplus \sigma_{\text{nlo},b}$$

$$\sigma_b^{\text{cor}} = \sigma_{\text{lum},b}$$

Random numbers:

$$r_b^{(e)}, r'^{(e)} \sim \mathcal{N}(0, 1)$$

SMEFT analysis: SMEFT asymmetry as a fit function

$$A_{\text{SMEFT},b} = \frac{\sigma_{\text{num},b}^{(0)} + \sum_{k=1}^{N_{\text{fit}}} C_k \sigma_{\text{num},b}^{(1)}}{\sigma_{\text{den},b}^{(0)} + \sum_{k=1}^{N_{\text{fit}}} C_k \sigma_{\text{den},b}^{(1)}}, \quad N_{\text{fit}} \in \text{Range}(7)$$

Linearization:

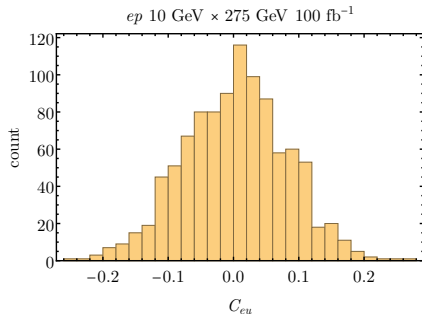
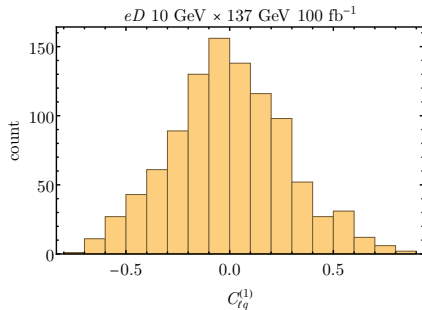
$$A_{\text{SMEFT},b} = A_{\text{SM},b} + \sum_{k=1}^{N_{\text{fit}}} C_k \delta A_{k,b}$$

This is the fit model on the pseudodata:

$$A_{\text{pseudo},b}^{(e)} = A_{\text{SM},b} + r_b^{(e)} \sigma_b^{\text{unc}} + r_b^{\prime(e)} \sigma_b^{\text{cor}}$$

$$\Rightarrow C_k \sim \mathcal{N}(0, \Delta C_k)$$

SMEFT analysis: SMEFT asymmetry as a fit function



SMEFT analysis: Best fits

χ^2 test statistic for each pseudoexperiment:

$$\chi^2^{(e)} = \sum_{b,b'=1}^{N_{\text{bin}}} [A_{\text{SMEFT},b} - A_{\text{pseudo},b}^{(e)}] H_{bb'} [A_{\text{SMEFT},b'} - A_{\text{pseudo},b'}^{(e)}]$$

$$H^{-1} = H_0^{-1} + H_{\text{pdf}}^{-1} : \text{total error matrix}$$

PDF errors:

$$(H_{\text{pdf}}^{-1})_{bb'} = \frac{1}{N_{\text{pdf}}} \sum_{m=1}^{N_{\text{pdf}}} (A_{\text{SM},m,b} - A_{\text{SM},0,b}) (A_{\text{SM},m,b'} - A_{\text{SM},0,b'})$$

PDF sets used: NNPDF3.1 NLO and NNPDFpo11.1

SMEFT analysis: Best fits

Polarimetry and **luminosity difference** can be limiting factors.

- ⇒ use data itself to constrain these systematic effects
- ⇒ simultaneous fits of C_k with **beam polarization**, P , and **luminosity difference**, A_{lum}

Fits of C_k with P :

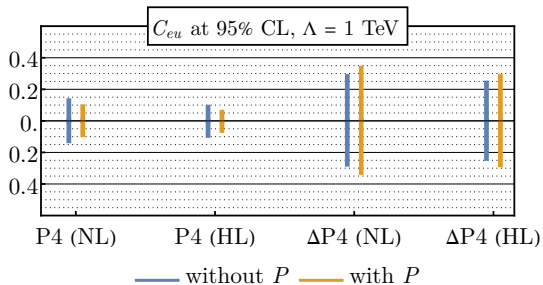
$$\chi^2(e) = \sum_{b,b'=1}^{N_{\text{bin}}} [PA_{\text{SMEFT},b} - A_{\text{pseudo},b}^{(e)}] \left[H_{bb'} \Big|_{\sigma_{\text{pol}} \rightarrow 0} \right] [PA_{\text{SMEFT},b'} - A_{\text{pseudo},b'}^{(e)}] + \frac{(P - \bar{P})^2}{\delta P^2}$$

Fits of C_k with A_{lum} :

$$\chi^2(e) = \sum_{b,b'=1}^{N_{\text{bin}}} [A_{\text{SMEFT},b} - A_{\text{pseudo},b}^{(e)} - A_{\text{lum}}] \left[H_{bb'} \Big|_{\sigma_{\text{lum}} \rightarrow 0} \right] [A_{\text{SMEFT},b'} - A_{\text{pseudo},b'}^{(e)} - A_{\text{lum}}]$$

SMEFT analysis: Fits with P

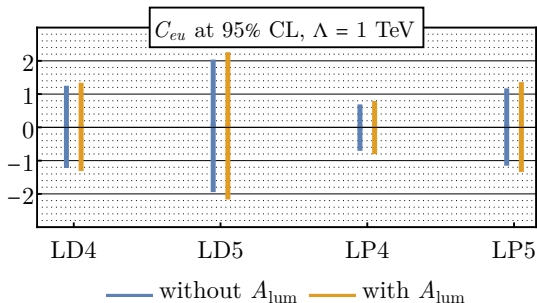
D4	0.82	-0.83	-0.82	0.83	-0.77	0.77	0.76
D5	0.66	-0.67	-0.67	0.67	-0.64	0.63	0.63
P4	0.83	-0.87	-0.79	0.86	-0.80	0.79	0.71
P5	0.71	-0.76	-0.68	0.75	-0.71	0.70	0.63
Δ D4	0.25	-0.25	-0.24	0.25	0.13	-0.14	-0.12
Δ D5	0.18	-0.18	-0.18	0.18	0.12	-0.12	-0.11
Δ P4	0.31	0.30	-0.31	0.31	0.14	0.06	-0.13
Δ P5	0.23	0.22	-0.23	0.22	0.14	0.07	-0.13
	C_{eu}	C_{ed}	C_{lq}^1	C_{lq}^3	C_{lu}	C_{ld}	C_{qe}



- 15 to 20% weaker bounds in **polarized** case
- 30 to 50% stronger bounds in **unpolarized** case
- Improvement is more significant than worsening \Rightarrow include P in the fits

SMEFT analysis: Fits with A_{lum}

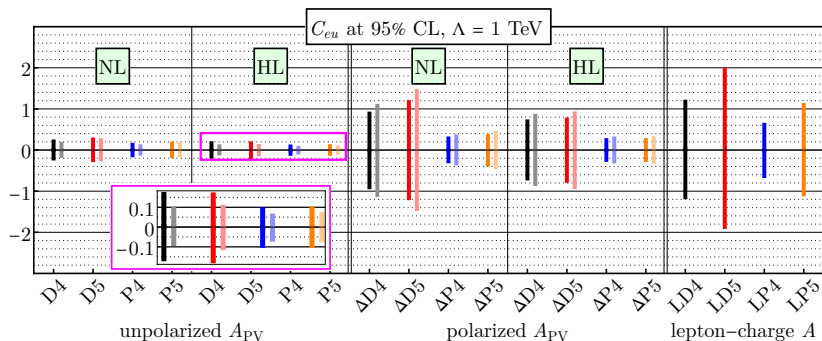
LD4	-0.50	0.50	-0.52	0.48	0.46	-0.46	0.44
LD5	-0.45	0.45	-0.47	0.42	0.38	-0.38	0.36
LP4	-0.36	0.41	-0.34	0.35	0.31	-0.35	0.30
LP5	-0.34	0.40	-0.32	0.33	0.27	-0.31	0.27
	C_{eu}	C_{ed}	C_{lq}^I	C_{lq}^S	C_{lu}	C_{ld}	C_{qe}



- 15 to 20% weaker bounds
- Significant worsening \Rightarrow don't include A_{lum} in the fits

SMEFT fit results

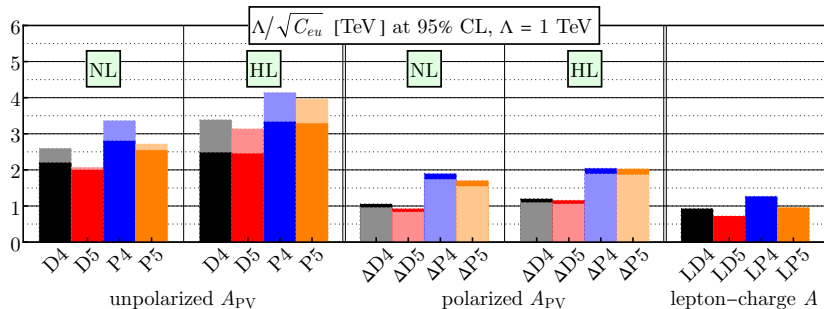
Single Wilson coefficients



In terms of the strength of bounds:

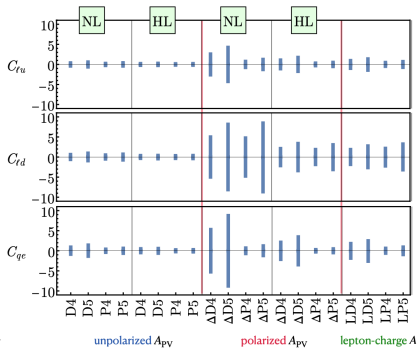
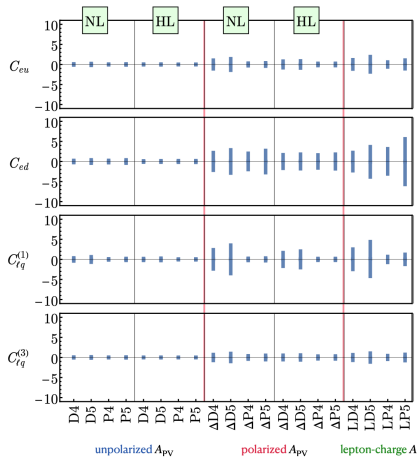
- proton > deuteron
- low-luminosity high-energy > high-luminosity low-energy
- unpolarized PV > polarized PV > lepton-charge
- unpolarized PV > polarized PV if NL \rightarrow HL
- improvement in bounds: HL > NL for unpolarized PV if with P

Single Wilson coefficients



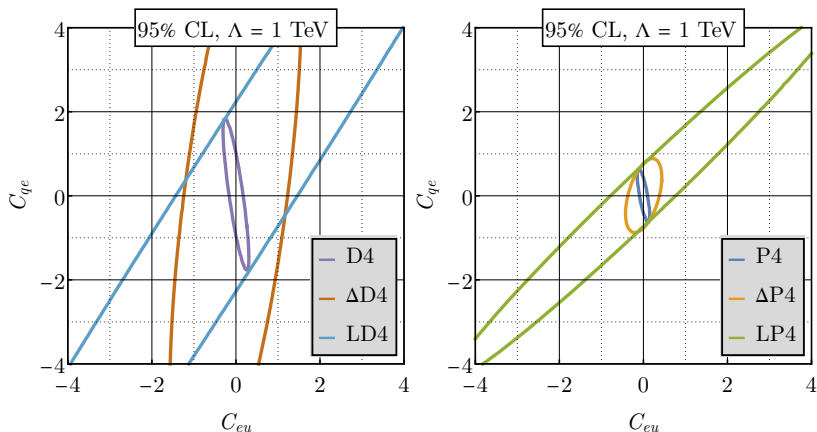
- UV scales ~ 3 TeV in NL case
- UV scales ~ 4 TeV in HL case

Single Wilson coefficients



Double Wilson coefficients

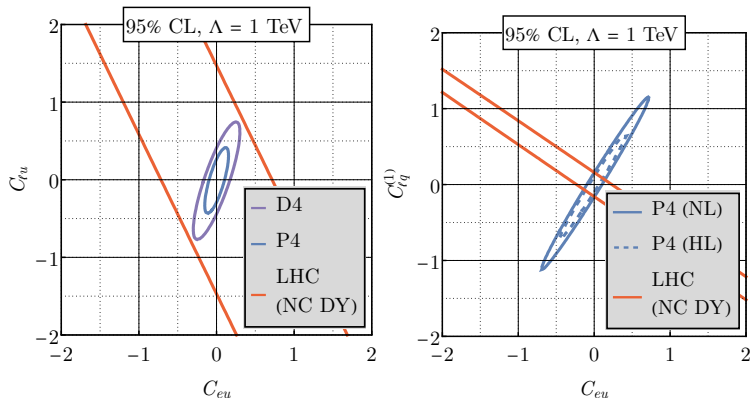
Compare the bounds from deuteron vs. proton data in the nominal-luminosity case for all the three types of asymmetries:



- The unpolarized PV asymmetries lead to strongest bounds.
- Proton data imposes stronger bounds.

Double Wilson coefficients

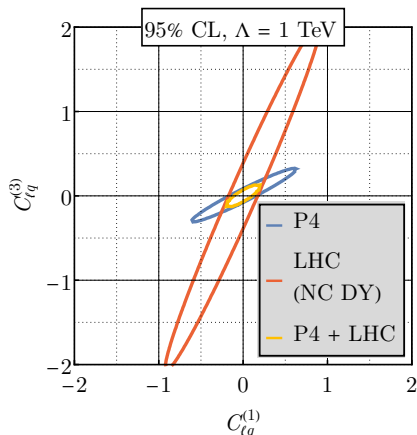
Compare the bounds from deuteron and proton data of **unpolarized** PV asymmetries to the 8-TeV 20-fb⁻¹ LHC NC DY data (Boughezal, Petriello, & Wiegand [[2004.00748](#), [2104.03979](#)]):



The LHC fits are highly degenerate and exhibit a flat direction, which remain even in the high-luminosity case. The EIC can resolve these and constrain this parameter space strongly.

Double Wilson coefficients

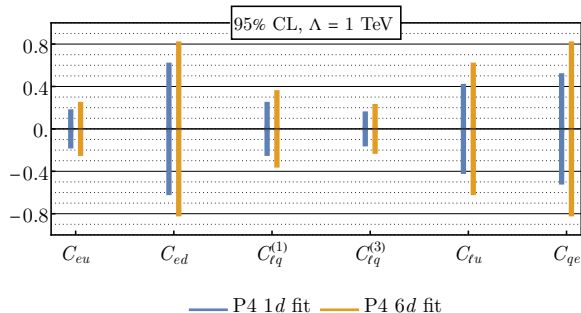
Compare proton data of **unpolarized** PV asymmetries to the 8-TeV 20-fb⁻¹ LHC NC DY data (Boughezal, Petriello, & Wiegand [2004.00748]) when the LHC fit doesn't have a flat direction:



When the LHC fit gives a strong bound without showing a flat direction, the EIC can constrain the same parameter space even more strongly.

Multiple Wilson coefficients

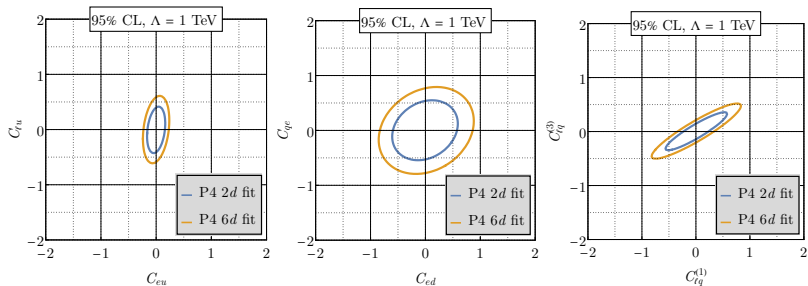
N_{fit}	N_{exp}
2	10^3
3	10^4
4	10^5
5	10^6
6	10^7
7	$10^8(?)!$



- **beam polarization** parameter, P , not included here
- 25 to 40% weaker bounds due to increased number of fitted parameters and correlations among them

Multiple Wilson coefficients

Compare the two-parameter fits of Wilson coefficients to the projections from a six-parameter fit:



- The $eeuu$ vertex contains the combination $C_{\ell q}^{(1)} - C_{\ell q}^{(3)}$ and the $eedd$ vertex has $C_{\ell q}^{(1)} + C_{\ell q}^{(3)}$.
- These may lead to degeneracies and flat directions in a multi-parameter fits of Wilson coefficients.
- The EIC can resolve this part of the parameter space, imposing strong bounds.

Conclusion

Philosophy and methodology

- We investigate the BSM potential of EIC in the model-independent SMEFT framework by focusing on semi-leptonic four-fermion operators at dimension 6 by giving a detailed accounting of uncertainties.
- We obtain bounds on Wilson coefficients from single-, double-, and even multiple-parameter fits by using techniques to simultaneously fit P and A_{lum} together with SMEFT parameters.

Findings

- We find that UV scales up to 3 TeV can be probed with nominal annual luminosity.
- This value becomes 4 TeV with a 10-fold luminosity upgrade.
- We observe that the strongest bounds come from **unpolarized** PV asymmetries of proton.
- EIC is shown to be complementary and competitive to LHC NC DY by
 - * equally or more strongly confining the Wilson coefficients;
 - * resolving the degeneracies observed in the LHC data.

EIC was designed as a QCD machine and it shows strong potential for BSM physics.

The End